The British Journal of Radiology, *85* (2012), e523–e529

A novel correction factor based on extended volume to complement the conformity index

F JIN, PhD, Y WANG, MD and Y-Z WU, MD

Department of Radiation Oncology, Chongqing Cancer Institute, Chongqing City, China

Objective: We propose a modified conformity index (MCI), based on extended volume, that improves on existing indices by correcting for the insensitivity of previous conformity indices to reference dose shape to assess the quality of high-precision radiation therapy and present an evaluation of its application.
Methods: In this paper, the MCI is similar to the conformity index suggested by Paddick ($CI_{Paddick}$), but with a different correction factor. It is shown for three cases: with an extended target volume, with an extended reference dose volume and without an extended volume. Extended volume is generated by expanding the original volume by 0.1–1.1 cm isotropically. Focusing on the simulation model, measurements of MCI employ a sphere target and three types of reference doses: a sphere, an ellipsoid and a cube. We can constrain the potential advantage of the new index by comparing MCI with $CI_{Paddick}$. The measurements of MCI in head–neck cancers treated with intensity-modulated radiation therapy and volumetric-modulated arc therapy provide a window on its clinical practice.
Results: The results of MCI for a simulation model and clinical practice are presented and the measurements are corrected for limited spatial resolution. The three types of MCI agree with each other, and comparisons between the MCI and $CI_{Paddick}$ are also provided.
Conclusion: The results from our analysis show that the proposed MCI can provide more objective and accurate conformity measurement for high-precision radiation therapy. In combination with a dose–volume histogram, it will be a more useful conformity index.

Received 18 April 2011
Revised 31 May 2011
Accepted 13 June 2011

DOI: 10.1259/bjr/27949149

Modern radiotherapy techniques include three-dimensional conformal radiation therapy [1–4], intensity-modulated radiation therapy [5–10] and image-guided radiation therapy [11, 12]. Current practice for radiation therapy involves optimisation of treatment plans using physical criteria (*i.e.* maximisation of target dose and minimisation of doses to critical structures). The evaluation of competing plans requires an in-depth analysis of isodose distributions.

Since Anderson [13] proposed the natural dose–volume histogram (DVH) in 1986, several dosimetric parameters for the description of the quality of radiation therapy application have been reported [14, 15], namely coverage index, external volume, relative dose homogeneity index, overdose volume index, sum index, uniformity index and volume gradient ratio [16]. Additionally, dose conformity indices, normal tissue complication probability (NTCP) and tumour control probability (TCP) were provided later. Conformity indices and outcome-based plan evaluations (NTCP, TCP) are also dependent on DVH analysis.

The conformity index was developed to score several competing plans for the same patient in order to choose the optimal one. In the past few years, several different indices have been reported to measure the conformity of the reference dose to the target volume. The conformity index was first recommended in 1993 by the Radiation Therapy Oncology Group (RTOG) [17] and described in Report 62 of the International Commission on Radiation Units and Measurements (ICRU) [18, 19]. It was defined as the ratio of the prescription isodose volume to the target volume. The RTOG guidelines defined a ratio of 1.0–2.0 as per the protocol, and ratios in the range of 0.9–1.0 and 2.0–2.5 as minor variations. A similar conformity index used by Knoos et al [20] was defined as the ratio of the planning target volume to the volume of the prescription isodose curve. Nedzi et al [21] used a conformity index called the treatment volume ratio, which was defined as the ratio of the target volume to the treatment volume. A modified conformity index (MCI) based on that of Nedzi et al was suggested by Paddick [22], who took into account the location of the prescription volume with respect to the target volume.

Although Paddick's conformity index $CI_{Paddick}$ has been widely adopted as a benchmark for assessing radiation therapy conformity and outcomes, it depends (just like other similar indices) on target size and shape, but is not sensitive to the reference isodose (ID_{ref}) shape in some special cases. This effect has not yet been thoroughly studied in the previous literature.

The objective of this paper is to systematically investigate the contribution of the shape of the (ID_{ref}) and target to the conformity index. We also propose an MCI

Address correspondence to: Professor Yong-Zhong Wu, Department of Radiation Oncology, Chongqing Cancer Institute, Chongqing City 400030, China. E-mail: jfazj@hotmail.com

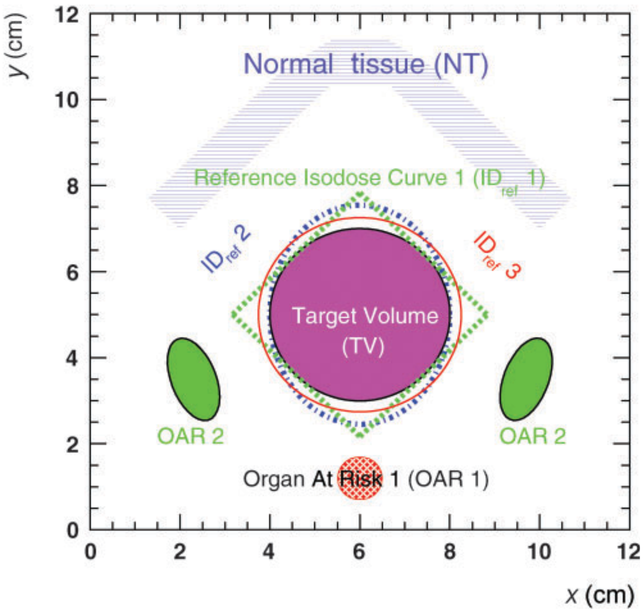

Figure 1. Schematic diagram of a typical head–neck cancer for computation of the conformity index. In this schematic diagram, the normal tissue, organs at risk, target volume and reference isodose curves are displayed.

based on $CI_{Paddick}$, which employs a correction factor to eliminate the shape insensitivity effect. Accordingly, the new conformity index is dependent on the (ID_{ref}) shape.

Methods and materials

Head and neck cancers comprise a diverse group of diseases, including malignancies of the oral cavity, oropharynx, larynx, sinuses and skull base. Treatment of these cancers includes a combination of surgical resection, chemotherapy and radiotherapy. Patients with head–neck and definitive brain tumours are routinely treated with intensity-modulated radiotherapy (IMRT) to enable delivery of highly conformal dose distribution to the tumour while sparing surrounding critical structures. The present article details simulation models and clinical data for patients with head–neck cancer treated with IMRT and volumetric-modulated arc therapy (VMAT).

Modelling and simulation

We create simulated ID_{ref} curves, target volume, normal tissue (NT) and organs at risk (OARs) to represent clinical practice. For one sphere target, three different shapes of ID_{ref} curves are simulated. These shapes include a sphere, an ellipsoid and a cube. In order to simplify the calculation, we measured two-dimensional projection images as shown in Figure 1. The target volume is a circle with radius 2.0 cm. The parameters of three ID_{ref} curves are listed in the Table 1.

The conformity index suggested by Paddick is calculated for each of the ID_{ref} curves. It is defined as

$$CI_{Paddick} = \frac{TV_{RI}}{TV} \times \frac{TV_{RI}}{V_{RI}}, \quad (1)$$

where TV_{RI} is the target volume covered by the ID_{ref}, V_{RI} is the volume of the ID_{ref} and TV is the target volume. The first fraction of this equation defines the quality of coverage of the target; the second fraction defines the volume of healthy tissue receiving a dose greater than or equal to the reference dose. $CI_{Paddick}$ ranges from 0.0 to 1.0, where 1.0 is the ideal value.

Table 1 shows that the three different ID_{ref} curves have the same volume and cover an equivalent target volume. According to Equation (1), all of the conformity indices are equal to 0.78, as shown in Table 1. The optimal radiation therapy cannot be depicted accurately with $CI_{Paddick}$ alone; however, there are another three ways in which the plan can be evaluated accurately, with which $CI_{Paddick}$ can be modified.

Correction factor from the target volume

If the ID_{ref} covers all of the clinical and pathological target volume, we can extend the target volume to find the optimal extended target volume (OETV) with the maximum value of $CI_{Paddick}$. On the other hand, if the ID_{ref} does not cover all of the clinical pathological target volume, we need to shrink the target volume to find the optimal target volume with the maximum value of $CI_{Paddick}$. The two types of analysis are similar. In our analysis, the extended target volume is adopted owing to our model seen in Figure 1.

An MCI is proposed based on extended target volume (ETV). It is defined as

$$MCI = \frac{ETV_{RI}}{ETV} \times \frac{ETV_{RI}}{V_{RI}} \times F_{ETV} \quad (2)$$

$$F_{ETV} = 1.0 - \frac{|ETV - TV|}{TV} \quad (3)$$

and

$$|ETV - TV| = \min(|OETV_1 - TV|, |OETV_2 - TV|, \ldots) \quad (4)$$

where $OETV_1$ is the OETV from the first plan and $OETV_2$ is from the second plan; ETV means the OETV closest to the target volume; ETV_{RI} is the ETV covered by the ID_{ref}; and F_{ETV} is the correction factor from the ETV. It depicts the distance between target volume and OETV. The correction factor F_{ETV} ranges from 0.0 to 1.0. When the ETV is the original target volume, the MCI becomes $CI_{Paddick}$.

Table 1. The model parameters of reference isodose curves for head–neck cancer

Sample	Length (cm)	Perimeter (cm)	Area (cm^2)	Area of overlap (cm^2)	Confirmity index
Circle	2.26 (radius)	14.18	16.00	12.56	0.78
Ellipse	2.00 (SA) 2.54 (LA)	14.75	16.00	12.56	0.78
Square	4.00 (side)	16.00	16.00	12.56	0.78

SA, short axis; LA, long axis.

Correction factor from the reference isodose

This method is similar to the ETV. The MCI is proposed based on the optimal extended isodose (OEI) with the maximum value of $CI_{Paddick}$. It is defined as

$$\mathrm{MCI} = \frac{\mathrm{TV_{EI}}}{\mathrm{TV}} \times \frac{\mathrm{TV_{EI}}}{V_{\mathrm{EI}}} \times \mathrm{F_{EI}} \qquad (5)$$

$$F_{\mathrm{EI}} = 1.0 - \frac{|V_{\mathrm{EI}} - V_{\mathrm{RI}}|}{V_{\mathrm{RI}}} \qquad (6)$$

and

$$|V_{\mathrm{EI}} - V_{\mathrm{RI}}| = \min(|V_{\mathrm{OEI1}} - V_{\mathrm{RI1}}|, |V_{\mathrm{OEI2}} - V_{\mathrm{RI2}}|, \ldots), \qquad (7)$$

where the subscripts indicate different plans; $\mathrm{TV_{EI}}$ is the target volume covered by the extended isodose, V_{EI} is the volume of the extended isodose and F_{EI} is the correction factor from the extended isodose. It depicts the distance between the $\mathrm{ID_{ref}}$ and the extended isodose. The correction factor F_{EI} ranges from 0.0 to 1.0. When the extended isodose is the $\mathrm{ID_{ref}}$, the MCI becomes $\mathrm{CI_{Paddick}}$.

Correction factor from the target surface

If we take into account the difference in surface area between the target and $\mathrm{ID_{ref}}$ in the MCI, the MCI is defined as

$$\mathrm{MCI} = \frac{\mathrm{TV_{RI}}}{\mathrm{TV}} \times \frac{\mathrm{TV_{RI}}}{V_{\mathrm{RI}}} \times F_{\mathrm{SA}} \qquad (8)$$

and

$$F_{\mathrm{SA}} = 1.0 - \frac{|\mathrm{SA_{RI}} - \mathrm{SA_{TV}}|}{\mathrm{SA_{TV}}} \qquad (9)$$

where $\mathrm{SA_{RI}}$ is the surface area of the $\mathrm{ID_{ref}}$, $\mathrm{SA_{TV}}$ is the surface area of the target volume and F_{SA} is the correction factor from the target surface. It depicts the difference in surface area between the $\mathrm{ID_{ref}}$ and the target volume. When $\mathrm{F_{SA}}$ is equal to 1.0, there is no difference between them, so it is an ideal case.

Clinical practice

Patients underwent CT scans with slice cuts of 5 mm thickness in the supine position. Structures were manually contoured onto the CT scan slices following the ICRU Report 50 recommendations [23]. The gross tumour volume and clinical target volume (CTV) were contoured on axial CT scan slices. The CTV included clinical and suspected subclinical involvement. The radiation dose was prescribed to a planning target volume, which was generated by expanding the CTV by 0.5–1.0 cm. Normal tissues and OARs were also entered onto the planning CT scan, such as brain stem, spinal cord, parotid gland and so on.

IMRT plans and VMAT were generated using commercial inverse planning software (Eclipse™ v. 8.6; Varine Corp., Palo Alto, CA). Dynamic multileaf collimators were used to shape the fields. Nine-field coplanar plans with equally spaced beams (the most prevalent beam arrangement found in the literature for head–neck IMRT) were used. For comparison purposes, another four different coplanar beam angle arrangements were examined. All IMRT plans used split beams to treat the primary and upper neck nodal regions. The first beam-angle configuration consisted of a simple 5-beam-angle arrangement (including one anterior field, 0°; two anterior–oblique fields, 65° and 130°; and two posterior–oblique fields, 230° and 295°) to test whether a reduction in the number of beams was feasible. The second was a 7-beam-angle arrangement selected by an experienced physicist (0°, 60°, 90°, 150°, 210°, 270° and 300°). The third was a posterior-weighted 7-beam-angle configuration (90°, 120°, 150°, 180°, 210°, 240° and 270°) based on a Memorial Sloan-Kettering technique described by Hunt et al [24]. The fourth configuration

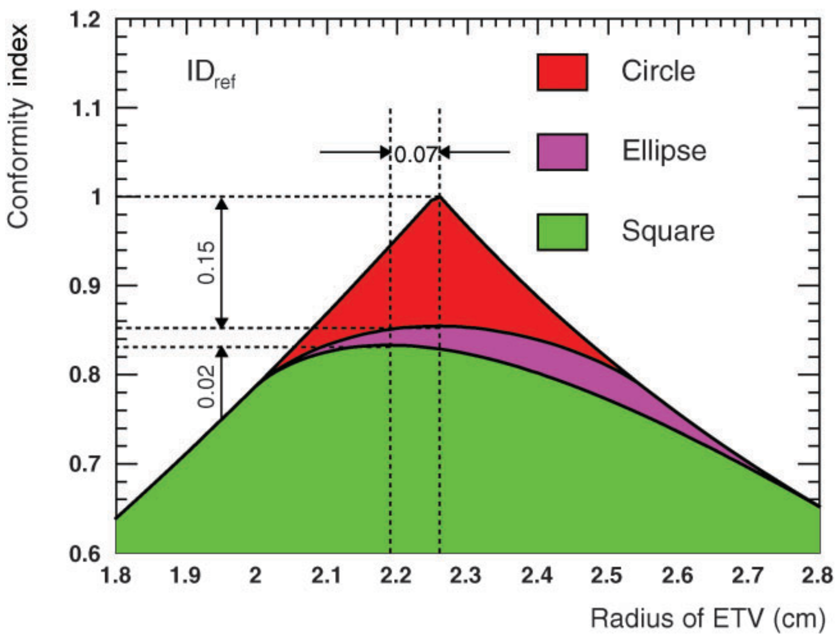

Figure 2. The conformity index of Paddick as a function of the radius of the extended target volume (ETV) for three types of reference isodose ($\mathrm{ID_{ref}}$). The maximum conformity index values are different in the three cases.

Table 2. The modified conformity indices (MCIs) based on the extended target volume (ETV) compared with the Paddick conformity index ($CI_{Paddick}$) for the three types of reference isodose

Sample	$CI_{Paddick}$ of OETV	F_{ETV}	MCI	$CI_{Paddick}$
Circle	0.94	0.80	0.75	0.78
Ellipse	0.85	0.80	0.68	0.78
Square	0.83	0.80	0.66	0.78

F_{ETV}, correction factor from the ETV; OETV, optimal extended target volume.

was an 8-beam-angle arrangement (0°, 30°, 90°, 130°, 230°, 260°, 290° and 330°). Additionally, three types of VMAT plans (*i.e.* one coplanar arc, two coplanar arcs and two non-coplanar arcs) were designed for the same patient. The dose–volume constraints of the target and normal tissues were defined for patients.

Structures were modelled as three-dimensional point clouds in Eclipse. Two important parameters can be changed: the number and resolution of the points in the point clouds. The point cloud generation algorithm places more points close to the structure's external surface to ensure proper representation of complex shapes. The resolution of the points is defined as the approximate distance between the points. The correction for effects of finite resolution is discussed in the following section.

Results

Simulation results

Correction factor from the target volume

To obtain an MCI with a correction factor from the ETV, the dependence of $CI_{Paddick}$ on the radius of the extended target for the three types of ID_{ref} is shown in Figure 2. Because the circle ID_{ref} has the same shape as the target volume, but with a different radius, $CI_{Paddick}$ of the OETV is unity. A sharp peak is observed in the $CI_{Paddick}$ spectrum of the circle ID_{ref}. The ellipse ID_{ref} has a higher $CI_{Paddick}$ of OETV 0.85, and the square has the lowest of 0.83. Additionally, the broadening effect of $CI_{Paddick}$ (namely the lower the $CI_{Paddick}$ of OETV is, the wider the spectrum of the conformity index becomes) is also observed. Circle and ellipse ID_{ref} values have the same OETV, but the square ID_{ref} has a smaller OETV. Comparing the three types of ID_{ref}, the OETV of the square ID_{ref} is adopted as the ETV.

The correction factors are calculated with Equation (3). The MCIs compared with $CI_{Paddick}$ are listed in Table 2. After modifying $CI_{Paddick}$, we find that the MCI can provide us with a precise index. The circle ID_{ref} has the highest MCI of 0.75, which is larger than the ellipse (0.68) and square (0.66).

Correction factor from the reference isodose

To calculate an MCI with a correction factor from the ID_{ref}, the dependence of $CI_{Paddick}$ on the geometric parameters of the optimal isodose is obtained for the three types of ID_{ref}. Using the correction factor, the MCIs are shown in Table 3. The circle ID_{ref} also has the highest MCI (0.79).

Correction factor from the target surface

The results of the MCIs with correction factors from the target surface are listed in Table 4. They are consistent with the previous methods. The circle ID_{ref} has the highest MCI (0.68).

In conclusion, the MCIs of three types of ID_{ref} are compared with $CI_{Paddick}$, shown in Figure 3. As can be seen, Paddick conformity indices are the same (0.78). After the correction factors are employed using the above methods, the MCI provides access to the optimal radiotherapy. The circle ID_{ref} always has the highest indices and the square one has the lowest indices. The results of the three methods are consistent.

Clinical results

Based on the structural model reconstructed by Eclipse, we extend and shrink the target volume to observe the change of $CI_{Paddick}$. As shown in Figure 4, the difference of margin of the target volume ranges from −1.1 to +0.5 cm. Red points represent the highest value of $CI_{Paddick}$. When target volumes are expanded, $CI_{Paddick}$ changes little. A line is used to fit to the highest value of $CI_{Paddick}$ of the ETV with the smallest χ^2 (the goodness of the fit), χ^2/degrees of freedom=0.0001/4. The parameters are listed in the top-right corner of Figure 4. The slope parameter is about 0.05. The $CI_{Paddick}$ of the ETV increases slowly with the decrease of volume and it achieves the maximum value when the ETV is the original target volume.

Figure 4 shows the dependence of $CI_{Paddick}$ on the choice of a reference dose. The dependence of $CI_{Paddick}$ on the ETV is also shown. In the following analysis, three reference doses (namely 80%, 90% and 100%) are discussed. Using Equations (2) and (5), the MCIs are calculated and compared with $CI_{Paddick}$. The results are listed in Table 5. MCI_{ETV} is the MCI with the correction factor from the ETV, and MCI_{OI} is the MCI with the correction factor from the extended reference isodose (ERI). Table 5 shows that the 90% ID_{ref} has the highest conformity index. They are 0.82,

Table 3. The modified conformity indices (MCIs) with a correction factor from the reference isodose (ID_{ref}) compared with Paddick conformity index ($CI_{Paddick}$) for the three types of ID_{ref}

Sample	$CI_{Paddick}$ of OI	F_{OI}	MCI	$CI_{Paddick}$
Circle	1.00	0.79	0.79	0.78
Ellipse	0.85	0.79	0.67	0.78
Square	0.40	0.79	0.32	0.78

F_{OI}, correction factor from the optimal isodose (OI).

Table 4. The modified conformity indices (MCIs) based on the surface area correction compared with the Paddick conformity index ($CI_{Paddick}$) for the three types of reference isodose

Sample	Perimeter	F_{SA}	MCI	$CI_{Paddick}$
Circle	14.18	0.87	0.68	0.78
Ellipse	14.75	0.82	0.64	0.78
Square	16.00	0.72	0.56	0.78

F_{SA}, correction factor from the surface area.

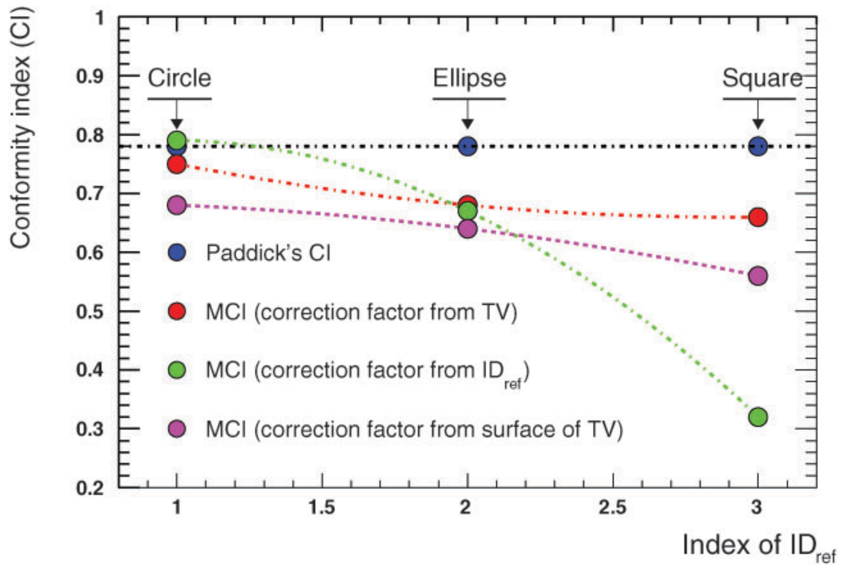

Figure 3. Comparison of the four conformity indices of three types of reference isodose (ID_{ref}). For the index of ID_{ref}, the value of 1 is for a circle, 2 is for an ellipse and 3 is for a square. MCI, modified conformity index; TV, target volume.

0.82 and 0.67 for the three types of conformity index separately. There is good agreement among $CI_{Paddick}$, MCI_{ETV} and MCI_{OI}. Until now, Eclipse has been unable to provide the surface area of the structure in their reconstructed model, so we do not discuss MCI_{SA} here.

Discussion

A correction for volume resolution from the dependence of the conformity index on the normalised relative dose is shown in Figure 5. In consideration of the volume resolution, the red points represent the conformity index with relative uncertainty 0.2% and blue ones with 10%. In order to separate the two cases, a factor of 0.9 is applied to the conformity index with relative uncertainty 10%. Polynomial fitting is performed. The highest conformity index can be obtained from polynomial curve fitting, and it is normalised to 1.0.

A shape comparison of the two polynomial curves is shown below the curves in Figure 5. A peak shift occurs in some cases. However, the majority of two curves agree with each other, except for the part of higher relative dose. A suitable confidence interval from 0.99 to 1.01 is considered the optimal conformity index range owing to the peak shift effect. The corresponding doses in this range are regarded as the optimal doses of the ETV, and the overlap between the ETV and the ID_{ref}.

For nine-field coplanar IMRT, the DVH of the ETV, ERI and the overlap between the ETV and ERI is shown in Figure 6. The bands represent the systematic uncertainty from the correction of volume resolution, and the dot-dashed line is the 95% ID_{ref} curve. The ETV and corresponding overlap with the same optimal dose constitute a pair. The gap between them decreases with the decrease of volume. When the volume is equal to $255.5\,cm^3$ (the value of the target volume), the smallest difference among ETV, ERI and the overlap between them is observed. That means there is the highest conformity index here. DVH plateaus of the ETV and overlap are formed when the volume is $<200\,cm^3$. The 95% dose covers the target well. As is known, the ETV

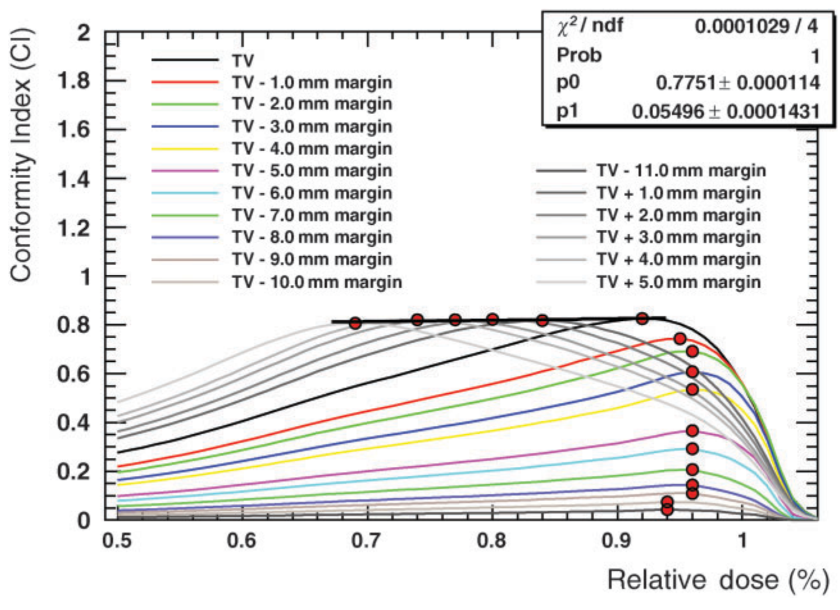

Figure 4. The conformity index (CI) of Paddick calculated according to Equation (1) depends on the choice of the reference dose. The relative doses are normalized to the prescription dose for the extended target volume (ETV). The red points represent the maximum Paddick CI of the ETV. df, degrees of freedom; Prob, probability; TV, target volume.

Table 5. Comparison of the conformity index of three reference doses (80%, 90% and 100%) between the Paddick conformity index ($CI_{Paddick}$) and the modified conformity index

Sample	$CI_{Paddick}$	MCI_{ETV}	MCI_{OI}
80%	0.70	0.70	0.66
90%	0.82	0.82	0.67
100%	0.56	0.56	0.52

MCI_{ETV}, modified conformity index based on extended target volume; MCI_{OI}, modified conformity index based on the optimal isodose.

and the overlap are in the midst of the original target volume. We find that there is a big difference between the ETV and ERI below 50 cm^3. It means high doses occur in the periphery of the target volume. The gradient of the dose can be measured using the right part of the ERI. A line fitting to them is performed.

In order to testify to the privileged role of the MCI in the evaluation of high-precision radiotherapy, several IMRT and VMAT curves were generated for the same data set. A template of planning dose constraints was constructed based on our previous planning experience in the Eclipse treatment planning system. For each patient, fine adjustment was required to achieve the treatment goals. The final results of the conformity indices are listed in Table 6 for one typical case. MCIs have different values from $CI_{Paddick}$. The VMAT plan with two non-coplanar arcs has the highest conformity indices from the calculation of three types of conformity index, but the MCI based on the optimal isodose shows a significant advantage: (MCI_{OI}=0.870)>($CI_{Paddick}$=0.827).

The evaluation of the optimal plan should take into account the quality of tumour irradiation, irradiation of non-critical healthy tissues and irradiation of critical organs. The first two parameters correspond to the MCI described above. It can be multiplied by other indices correlated with the various critical organs to assess the conformal degree of a plan comprehensively.

Conclusions

Because the conformity index could facilitate decisions during analysis of various treatment plans proposed for

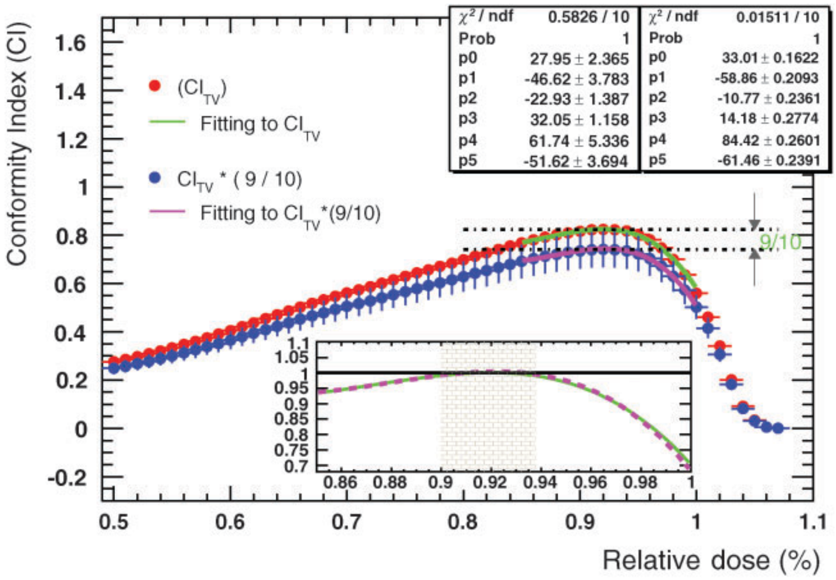

Figure 5. The correction for volume resolution in the calculation of conformity index (CI) as a function of normalised relative dose. Polynomial curves are fitted to the CI spectrum. CI_{TV}, target volume conformity index; df, degrees of freedom.

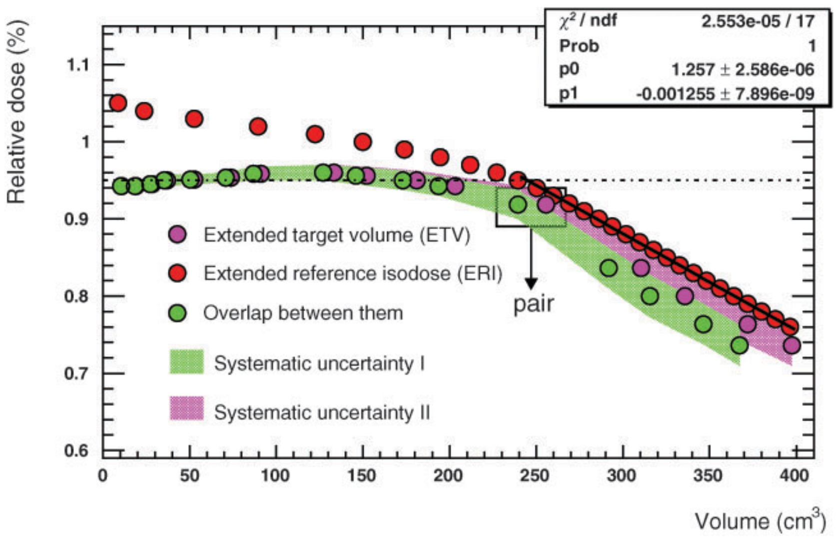

Figure 6. The dose–volume histogram (DVH) comparison among extended target volume, extended reference isodose (ERI) and the overlap between them. The gradient of the dose is measured by fitting to the DVH of the ERI. df, degrees of freedom.

Table 6. The comparison of the conformity index from different plans between the conformity index of Paddick ($CI_{Paddick}$) and the modified conformity index

Sample	$CI_{Paddick}$	MCI_{ETV}	MCI_{OI}
Case 1	0.790	0.793	0.806
Case 2	0.807	0.807	0.813
Case 3	0.816	0.816	0.827
Case 4	0.812	0.814	0.819
Case 5	0.820	0.817	0.838
Case 6	0.819	0.816	0.832
Case 7	0.823	0.834	0.862
Case 8	0.827	0.844	0.870

IMRT, intensity-modulated radiation therapy; MCI_{ETV}, modified conformity index based on the extended target volume; MCI_{OI}, modified conformity index based on the optimal isodose; VMAT, volumetric-modulated are therapy.

Case 1: five-field coplanar IMRT; case 2: seven-field coplanar IMRT; case 3: eight-field coplanar IMRT; case 4: posterior-weighted seven-field coplanar IMRT; case 5: nine-field coplanar IMRT; case 6: one-arc VMAT; case 7: VMAT with two coplanar arcs; case 8: VMAT with two non-coplanar arcs.

conformal radiotherapy and comparison between various available techniques, it is widely used in the study of the arrangement of optimal conformal radiotherapy. It is an attractive tool.

The insensitivity of previous conformity indices on the ID_{ref} in some cases is observed. The MCI, as described above, can offer objective and accurate measurements to evaluate high-precision radiotherapy. To date, existing treatment planning system software does not take into account the surface area difference between the target volume and ID_{ref}. The most simple MCI with a correction factor from the surface cannot be adopted in routine analysis. Planning software should be improved with regard to this problem, and our future work will take this into account.

References

1. Fukunaga-Johnson N, Sandler HM, McLaughlin PW, Strawderman MS, Grijalva KH, Kish KE, et al. Results of 3D conformal radiotherapy in the treatment of localized prostate cancer. Int J Radiat Oncol Biol Phys 1997;38:311–17.
2. Fukunaga-Johnson N, Sandler HM, Marsh R, Martel MK. The use of 3D conformal radiotherapy (3D CRT) to spare the cochlea in patients with medulloblastoma. Int J Radiat Oncol Biol Phys 1998;41:77–82.
3. Tinger A, Michalski JM, Cheng A, Low DA, Zhu R, Bosch WR, et al. A critical evaluation of the planning target volume for 3-D conformal radiotherapy of prostate cancer. Int J Radiat Oncol Biol Phys 1998;42:213–21.
4. Singh AK, Lockett MA, Bradley JD. Predictors of radiation-induced esophageal toxicity in patients with non-small-cell lung cancer treated with three-dimensional conformal radiotherapy. Int J Radiat Oncol Biol Phys 2003;55:337–41.
5. Seung S, Bae J, Solhjem M, Bader S, Gannett D, Hansen EK, et al. Intensity-modulated radiotherapy for head-and-neck cancer in the community setting. Int J Radiat Oncol Biol Phys 2008;72:1075–81.
6. Gomez DR, Zhung JE, Gomez J, Chan K, Wu AJ, Wolden SL, et al. Intensity-modulated radiotherapy in postoperative treatment of oral cavity cancers. Int J Radiat Oncol Biol Phys 2009;73:1096–103.
7. Vargas C, Fryer A, Mahajan C, Indelicato D, Horne D, Chellini A, et al. Dose–volume comparison of proton therapy and intensity-modulated radiotherapy for prostate cancer. Int J Radiat Oncol Biol Phys 2008;70:744–51.
8. Tham IW, Hee SW, Yeo RM, Salleh PB, Lee J, Tan TW, et al. Treatment of nasopharyngeal carcinoma using intensity-modulated radiotherapy—The National Cancer Centre Singapore experience. Int J Radiat Oncol Biol Phys 2009; 75:1481–6.
9. Miles EF, Larrier NA, Kelsey CR, Hubbs JL, Ma J, Yoo S, et al. Intensity-modulated radiotherapy for resected mesothelioma: the Duke experience. Int J Radiat Oncol Biol Phys 2008;71:1143–50.
10. Nath SK, Sandhu AP, Rose BS, Simpson DR, Nobiensky PD, Wang JZ, et al. Toxicity analysis of postoperative image-guided intensity-modulated radiotherapy for prostate cancer. Int J Radiat Oncol Biol Phys 2010;78:435–41.
11. Hatano K, Narita Y, Sakai M, Araki H. IGRT for cervical cancer: is it less toxic than non IGRT. Int J Radiat Oncol Biol Phys 2004;60:S486–7.
12. de Crevoisier R, Pommier P, Bachaud J, Crehange G, Boutry C, Chauvet B, et al. Image-guided radiation therapy (IGRT) in prostate cancer: preliminary results in prostate registration and acute toxicity of a randomized study. Int J Radiat Oncol Biol Phys 2009;75(Suppl. 1):S99.
13. Anderson, L. A ''natural'' volume-dose histogram for brachytherapy. Med Phys 1986;13:898–903.
14. van der Laarse R, Prins TPE. Comparing the stepping source dosimetry system and the Paris system using volume-dose histograms of breast implants. In: Mould RF, Battermann JJ, Martinez AA, Speiser BL, eds. Brachytherapy from radium to optimization. Veenendaal, The Netherlands: Nucletron; 1994. pp. 352–72.
15. Meertens H, Borger J, Steggerda M. Evaluation and optimization of interstitial brachytherapy dose distribution. In: Mould RF, Battermann JJ, Martinez AA, Speiser BL, eds. Brachytherapy from radium to optimization. Veenendaal, The Netherlands: Nucletron; 1994. pp. 300–6.
16. Baltas D, Kolotas C, Geramani K, Mould RF, Ioannidis G, Kekchidi M, et al. A conformity index (COIN) to evaluate implant quality and dose specification in brachytherapy. Int J Radiat Oncol Biol Phys 1998;40:515–24.
17. Shaw E, Kline R, Gillin M, Souhami L, Hirschfeld A, Dinapoli R, et al. Radiation Therapy Oncology Group: radiosurgery quality assurance guidelines. Int J Radiat Oncol Biol Phys 1993;27:1231–9.
18. ICRU. Prescribing, recording and reporting photon beam therapy (supplement to ICRU Report 50). Report 62. Washington, DC: International Commission on Radiation Units and Measurements; 1999.
19. Feuvret L, Noël G, Mazeron JJ, Bey P. Conformity index: a review. Int J Radiat Oncol Biol Phys 2006;64:333–42.
20. Knoos T, Kristensen I, Nilsson P. Volumetric and dosimetric evaluation of radiation treatment plans: radiation conformity index. Int J Radiat Oncol Biol Phys 1998;42:1169–76.
21. Nedzi LA, Kooy HM, Alexander E 3rd, Svensson GK, Loeffler JS. Dynamic field shaping for stereotactic radiosurgery: a modeling study. Int J Radiat Oncol Biol Phys 1993;25:859–69.
22. Paddick II. A simple scoring ratio to index the conformity of radiosurgical treatment plans. Technical note. J Neurosurg 2000;93:219–22.
23. ICRU. Prescribing, recording and reporting photon beam therapy. Report 50. Washington, DC: International Commission on Radiation Units and Measurements; 1994.
24. Hunt MA, Zelefsky MJ, Wolden S, Chui C-S, LoSasso T, Rosenzweig K, et al. Treatment planning and delivery of intensity-modulated radiation therapy for primary nasopharynx cancer. Int J Radiat Oncol Biol Phys 2001;49(Suppl. 3):623–32.